

Shear-Rate, Concentration, Molecular Weight, and Temperature Viscosity Dependences of Hyaluronate, a Wormlike Polyelectrolyte

Eric Fouissac, Michel Milas,* and Marguerite Rinaudo

Centre de Recherches sur les Macromolécules Végétales, Affiliated with the Joseph Fourier University of Grenoble, B.P. 53 X, 38041 Grenoble Cedex, France

Received December 23, 1992; Revised Manuscript Received September 13, 1993*

ABSTRACT: The shear flow of hyaluronate solutions are studied on well characterized samples from bacterial sources. The dependence of the zero-shear viscosity, η_0 , with polymer concentration, molecular weight, and temperature are discussed. The behavior of this semirigid ionic polymer differs, in some way, from that of flexible polymers in solution. In particular, the slope of the plot of $\log \eta_0$ vs $\log M$ at fixed polymer concentration, C , is equal to 4 instead of 3.4 in the more concentrated domain. Nevertheless the concentration dependences of η_0 have been analyzed on the basis of models developed for flexible polymers and polyelectrolytes. These models seem to apply to wormlike polymers with a presence of a limited semidilute region. The onset of shear thinning is found to be well characterized from the inverse of the longest relaxation time (τ_1^{-1}) in the solution taking into account C , M , and T dependences. The differences with hyaluronates of animal sources are attributed to the protein content in these samples.

Introduction

Hyaluronic acid is a water soluble glycosaminoglycane. Its primary structure consists of repeating disaccharide units of D-glucuronic acid and N-acetyl-D-glucosamine with $\beta(1\rightarrow4)$ interglycosidic linkages. It occurs in many living substrates as synovial fluid, vitreous humour, rooster comb, and umbilical cord. Indications of pharmacological activity have been demonstrated in the treatment of inflammatory and degenerative joint diseases^{1,2} and hyaluronate is used to replace the vitreous fluid during ophthalmic surgery,³ as examples of present applications. Therefore, increasing interest in the industrial production of hyaluronate is due not only to its potential application in cosmetic⁴ but also to the possibility of producing bacterial hyaluronate from *Streptococcus zoopidemicus*. In these applications, the rheological properties of hyaluronate solutions are important, especially their viscoelasticity, which plays an important role in some biological functions. More, over the past few years, there has been a growing interest in experimental and theoretical results concerning the solution properties of polyelectrolytes in relation to their apparent persistence lengths⁵⁻⁹ or more generally to the behavior of semirigid polymers in solution. It appears that if the rheological behavior of flexible¹⁰⁻¹⁴ and rigid^{12,15-17} polymers in solution is well described, it is not the case for semirigid polymers and polyelectrolytes in semidilute and concentrated regimes.¹⁸⁻²¹

Then rheological studies on hyaluronates are interesting not only due to their potential applications but also because this polymer behaves as a semirigid polyelectrolyte in solution. Up to now few studies have been reported on the flow properties of hyaluronate in solution²²⁻²⁶ and/or the range of polymer concentrations, molecular weights, were limited. More, in these investigations animal hyaluronates were used and the proteins present in these samples^{27,28} are responsible for aggregation which can perturb the rheological behavior.

In this work, we present viscosity data for aqueous solutions of sodium hyaluronate with added salt. Hyaluronate is a wormlike ionic macromolecule characterized

Table I. Molecular Characterization of the Hyaluronate Samples Used, in 0.1 M NaCl

sample	$10^{-5} M_w$	$[\eta]$ (mL/g)	k'	$\langle \rho^2 \rangle_z^{1/2}$ (Å)	$10^4 C^*$ (g/mL)	$10^3 C_c^*$ (g/mL)	$C_c^*[\eta]$	$\frac{C_c^*}{C^*}$
H-1	22	3400	0.44	1631	2	1.1	3.9	5.5
H-2	13.5	2300	0.57	1247	2.76	1.5	3.4	5.43
H-3	10	1850	0.51	1035	3.58	2.1	3.9	5.86
H-4	5	950	0.57	723	5.24	3.75	3.6	7.15
H-5	3.5	750	0.33	594	6.62	6	4.5	9.1

* Critical overlap concentration $C^* = 3M/4\pi N_A \langle \rho^2 \rangle^{3/2}$.

by an intrinsic persistence length ranging from 45 to 90 Å.²⁸⁻³⁰ Therefore, it shows the behavior of a wormlike polymer perturbed by ionic effects; the polyelectrolyte properties of this polymer were widely studied in a recent work³⁰ and will not be reconsidered here.

In this study, we use well-characterized hyaluronate samples from bacterial sources with molecular weights in the range 3.5×10^5 to 2.2×10^6 and report viscosity data over dilute through concentrated regions. The use of bacterial hyaluronates avoids the presence of aggregates in solution in comparison with animal hyaluronates.^{27,28} The ionic strength is maintained at 0.1 M in order to screen the long range electrostatic repulsions.

Experimental Section

Materials. Bacterial Na-hyaluronates with different molecular weights were produced by ARD Co. (Paris, France). The protein content was determined to be less than 0.1 % by weight. The characterization of the polymers, e.g. the molecular weight distribution and the weight average molecular weight, was performed on hyaluronate solutions (5×10^{-4} g/mL) in 0.1 M NH_4NO_3 by steric exclusion chromatography, using multidetection equipment previously described.³¹ The polydispersity of the different samples is $M_w/M_n \sim 1.3$. Some molecular characteristics of the samples used in this work are listed in Table I. To obtain a perfect dissolution, aqueous hyaluronate solutions were prepared using the following procedure: a hyaluronate sample for which the hydration degree was determined separately using a Setaram thermobalance G 70 (France) was dissolved in pure water and stirred at about 25 °C overnight. Then 1 M aqueous NaCl was added to the solutions to reach 0.1 M NaCl concentration. Different polymer concentrations have been also obtained by dilution with 0.1 M NaCl solution.

Measurements. Flow curves were obtained with two rheometers: the Contraves low-shear, LS 30, covering a shear-

* To whom correspondence should be addressed.

• Abstract published in *Advance ACS Abstracts*, November 1, 1993.

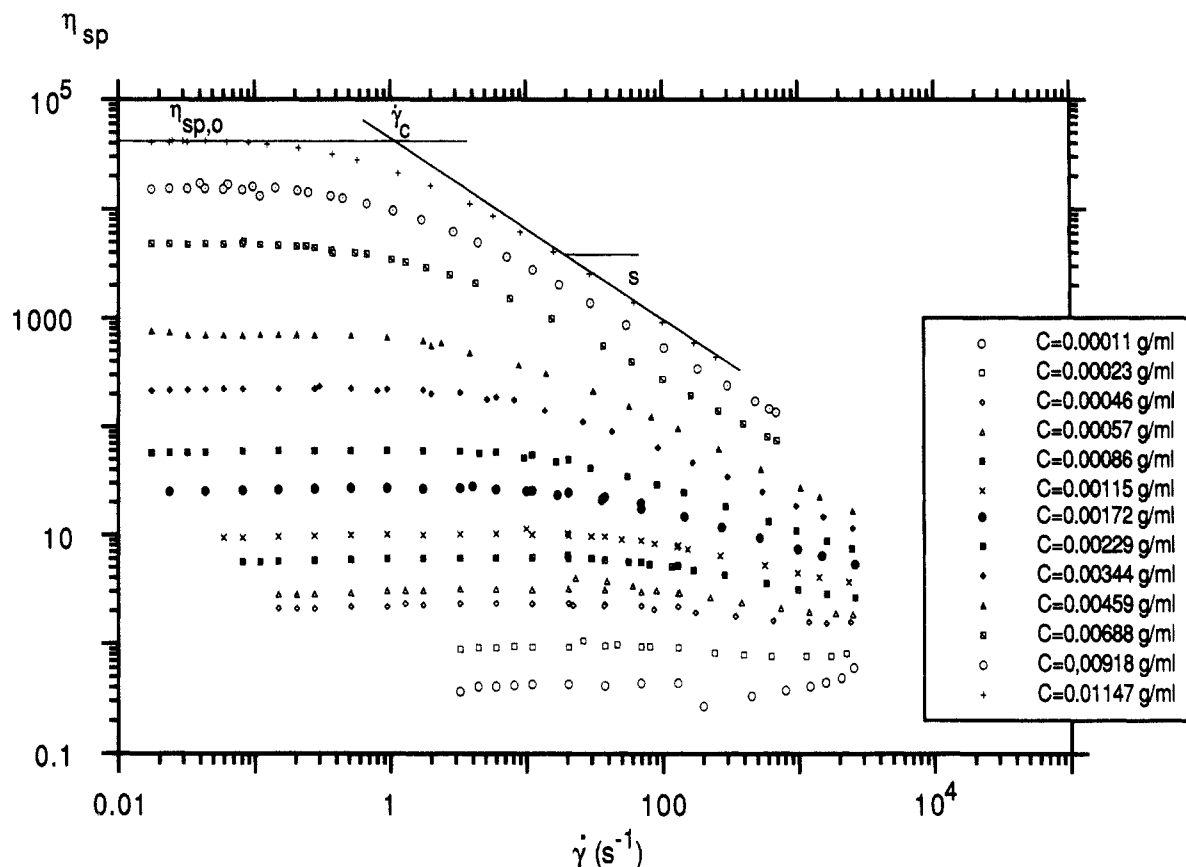


Figure 1. Influence of shear rate on the specific viscosity of H-1 at different polymer concentrations in 0.1 M NaCl at 25 °C.

rate ($\dot{\gamma}$) range from 0.017 to 128 s⁻¹ and the Carrimed CS 50 equipped with a Rheo 1000 C system and a 5.0 software which allows direct viscosity-shear-rate determination by angular speed control. The various geometries used were cones: 4- and 6-cm diameters 4° cone angle, 6-cm diameter 1° cone angle. The shear stress can be varied, depending upon the geometry used, from 0.005 to 3000 N m⁻², and then the corresponding shear rate, from 0.1 to 2800 s⁻¹, depending on the experimental conditions. For temperature measurements higher than 25 °C a solvent trap system from Carrimed was used.

Results and Discussion

The viscosity of polymer solutions is a particularly valuable property of molecular size and interactions. For example, the concentration dependence in a logarithmic plot of Newtonian specific viscosity ($\eta_{sp,0}$) for polymer solutions shows different behaviors depending on the range of polymer concentration. Increasing the polymer concentration, we can define the dilute, the semidilute, and the concentrated domains. The semidilute regime is very limited, and its rheological behavior is controlled by the degree of chain overlapping. In the concentrated domain, the distribution of segments in the solution is uniform; the chains then reach unperturbed dimensions.³² Critical concentrations C_c^* and C_c^{**} characterize the boundary between these domains.

Moreover, in the polymer melts it was found that, below a critical molecular weight M_c , $\eta_0 \propto M$ and, above M_c , $\eta_0 \propto M^{3-3.4}$. These power laws hold in concentrated solutions of flexible polymers^{10,11,33,34} although critical molecular weight depends on concentration. In many systems, the transition remains fairly well defined and, within the accuracy of the data, conforms to

$$(M_c)_{sol} = \frac{\rho}{C} M_c = \frac{M_c}{\phi} \quad (1)$$

where $(M_c)_{sol}$ is the molecular weight at which chain

entanglements become important at the concentration C , M_c is the value for undiluted polymer, ρ is the polymer volumic mass (1.6 g/mL), and ϕ is the volume fraction of polymer in solution. From this equation, the transition is expected to take place for different concentrations and molecular weights at the same value of the parameter CM .

In fact, the literature on viscosity related to low and high polymer concentrations behavior suggest two fundamentally different types of intermolecular interactions and parameters.¹⁰ The viscosity behavior at low concentrations is similar to that of a suspension of discrete particles. The interactions seem to depend upon the volume occupied by the molecules or alternatively upon the degree of overlap of the chains which can be estimated from the parameter $C[\eta]$. A second source of interactions, i.e. segment-segment contacts between molecules, has been considered in more concentrated solutions where free draining flow is assumed to dominate. In this, the relevant crossover parameter is related to the number of intermolecular contacts per molecule which is proportional to CM . It is interesting to note that this parameter emerges in the description of the crossover from the dilute to semidilute regime of static properties.

Behavior in the Newtonian Domain. Concentration and Molecular Weight Dependences. The flow curves were examined first at 25 °C. An example of a double-logarithmic plot of the specific viscosity η_{sp} vs shear rate $\dot{\gamma}$ for sample H-1 at different concentrations is shown in Figure 1. These curves can be characterized by three parameters: the "zero-shear" or Newtonian specific viscosity ($\eta_{sp,0}$), the critical shear rate corresponding to the onset of the shear thinning behavior ($\dot{\gamma}_c$), and the slope (s) of the curve in the shear dependent viscosity domain which characterize the pseudoplastic behavior of hyaluronate solutions together with $\dot{\gamma}_c$.

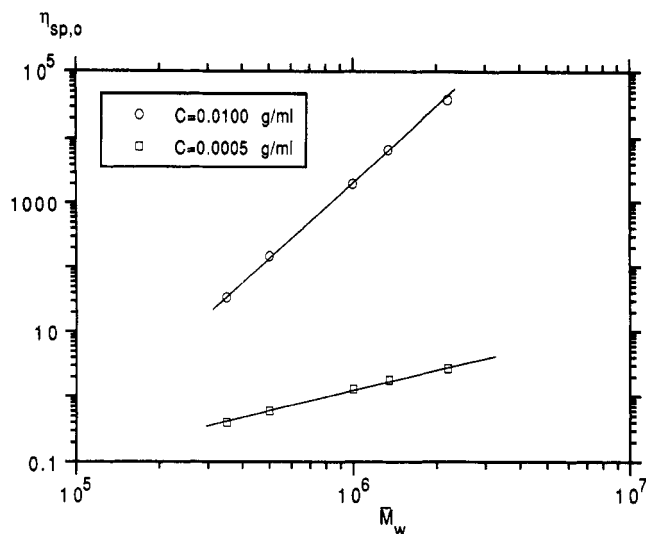


Figure 2. Variation of $\eta_{sp,0}$ at $C = 5 \times 10^{-4}$ g/mL (dilute regime) and $C = 0.01$ g/mL (semidilute regime) with the weight average molecular weight of hyaluronate samples in 0.1 M NaCl at 25 °C.

Table II. Dependence of $\eta_{sp,0}$ with the Concentration in the Dilute ($\eta_{sp,0} \propto C^\alpha$) and Concentrated Regimes ($\eta_{sp,0} \propto C^\beta$) in 0.1 M NaCl at 25 °C

sample	α	β	sample	α	β
H-1	1.21	4.2	H-4	1.19	4.0
H-2	1.24	4.1	H-5	1.15	3.8
H-3	1.24	4.1			

For each sample, a double-logarithmic plot of $\eta_{sp,0}$ against C shows two limiting behaviors at the lowest and highest concentrations, corresponding in this representation to quasi linear change of $\log \eta_{sp,0}$ vs $\log C$. These two limiting behaviors correspond respectively to the dilute and semidilute or moderately concentrated regimes.^{35,36} The values of the slopes of these average concentration dependences are given in Table II. In the dilute regime it is found $\eta_{sp,0} \propto C^{1.20 \pm 0.05}$ and in the more concentrated one $\eta_{sp,0} \propto C^{4.0 \pm 0.2}$ for the molecular weights used in this work.

Figure 2 shows double-logarithmic plots of $\eta_{sp,0}$ vs M_w in 0.1 M NaCl solutions at $C = 5 \times 10^{-4}$ and 10^{-2} g/mL. The figure reveals that the molecular weight dependence of $\eta_{sp,0}$ in 0.1 M NaCl solutions is given by $\eta_{sp,0} \propto M^4$ in the more concentrated regime and $\eta_{sp,0} \propto M$ in the dilute regime. We have checked that these exponents do not depend on the concentrations chosen in the different regimes for their determination.

Considering the Mark-Houwink exponent ($a = 0.80$)^{30,37} relating the intrinsic viscosity and the molecular weight in 0.1 M NaCl (Table I), it gives

$$\eta_{sp,0} \propto C^{1.2} M^{1.0} \quad \text{or} \quad (C[\eta])^{1.2} \quad (2)$$

$$\eta_{sp,0} \propto C^4 M^4 \quad \text{or} \quad (CM)^4 \quad (3)$$

The relations found in this work indicate that the viscosity depends on $C[\eta]$ (relation 2) at low concentrations in the dilute regime and CM at higher concentrations (relation 3) in the more concentrated regime. Thus a single curve $\log \eta_{sp,0}$ vs $\log C[\eta]$ is expected at lower concentrations and $\log \eta_{sp,0}$ vs $\log CM$ at higher concentrations. These representations are given in Figures 3 and 4 in 0.1 M NaCl. The dependence of $\log \eta_{sp,0}$ on $C[\eta]$ or CM in the dilute regime looks equally good from these figures due in fact to the high values of the Mark-Houwink exponent " a "

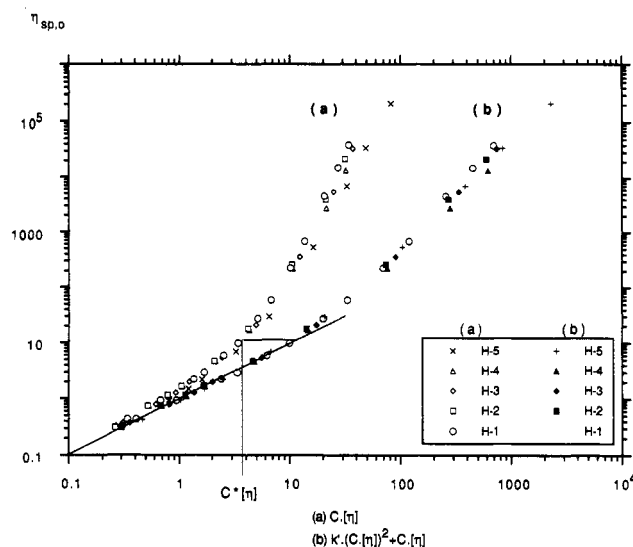


Figure 3. Dependence of $\eta_{sp,0}$ versus (a) $C[\eta]$ and (b) $C[\eta] + k'(C[\eta])^2$ for the different hyaluronates in 0.1 M NaCl at 25 °C.

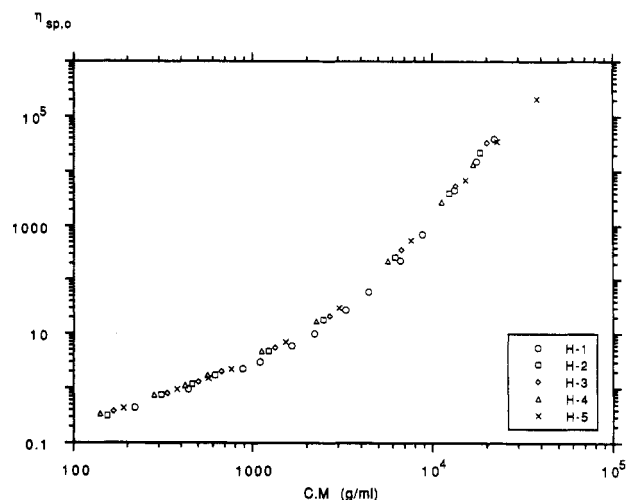


Figure 4. Dependence of $\eta_{sp,0}$ versus CM for the different hyaluronates in 0.1 M NaCl at 25 °C.

relating $[\eta]$ to M (relation 2; exponents 1 and 1.2 are difficult to separate).

As suggested previously,¹⁹ the critical concentration C_c^* that characterizes the end of the dilute regime can be expressed by the departure of the curve $\log \eta_{sp,0}$ vs $\log [C[\eta] + k'(C[\eta])^2]$ from the slope 1 characterizing the dilute regime where the Huggins law applies (Figure 3); the critical concentration obtained from hydrodynamic behavior is $C_c^*[\eta] = 3.8$ independent of the molecular weight in 0.1 M NaCl. The value of $C_c^*[\eta]$ determined from Figure 3 is an average value in good agreement with separate determinations for each molecular weight (Table I). The values of $C_c^*[\eta]$ found are larger than the theoretical predictions based on space filling considerations.^{10,22,32,38} C_c^* determined from the viscosity measurements must be quite different from the usual static overlap concentration $C^* \sim M/(\rho^2)^{3/2}$ determined from the radius of gyration given by light scattering. Takahashi et al.³⁵ found $C_c^*/C^* \sim 10$ for poly(α -methylstyrene) in a good solvent. This ratio is in the same range as found in this work (Table I) despite the difference in the C_c^* determination. Nevertheless $C_c^*[\eta]$ is in agreement with values found on other polysaccharides^{38,39} except for xanthan,¹⁹ succinoglycan,⁴⁰ and welan⁴¹ for which a value near 1 is obtained. The difference may be due to a higher stiffness of these last polysaccharides and/or intermolecular associations in solution. In comparison with previous results on hyalu-

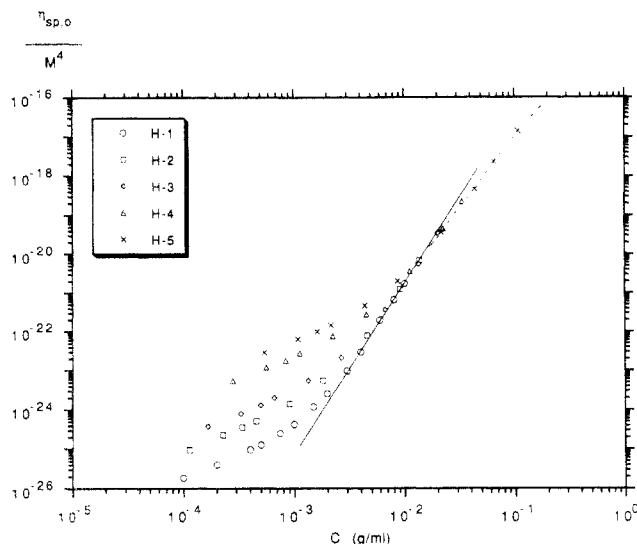


Figure 5. Plots of $\log(\eta_{sp0}/M^4)$ vs $\log C$ for the different hyaluronates in 0.1 M NaCl at 25 °C. The solid line denotes eq 9 of ref 35 ($\eta_{sp0}/M^4 \sim C^{4.35}$), and the dashed line, the concentrated region ($\sim C^{3.8}$).

ronates,²² the end of dilute behavior was found to occur at a higher $C[\eta]$ value (3.8 instead of 2.5²²). This difference cannot be attributed to the difference in the concentration of external salt (0.1 M instead of 0.15 M²²) nor to the method used for its determination. It may be due to the contribution of interchain associations occurring with hyaluronate from an animal source.

These results show that two different molecular weight dependences of viscosity characterize the dilute and the more concentrated regimes. In the dilute regime $\eta_0 \propto M$ which is similar to the result found in the melt for $M < M_c$ (or concentrated solutions for $C(M_c)_{sol} < \rho M_c$); in the more concentrated regime $\eta_0 \propto M^4$. In this domain the molecular weight exponent is higher than that found in the melt and concentrated solutions of flexible polymers for which exponents of 3 or 3.4 are observed experimentally^{10,13,21} and predicted theoretically.^{10,33} However, in some cases^{19,20} for semirigid polymers this exponent exceeds 3.4. For hyaluronates, Yanaki and Yamaguchi⁴³ claim a 3.4 power dependence of η_0 vs \bar{M}_v . But in their work the molecular weight determination is questionable using a Mark-Houwink relation obtained on hyaluronates from animal sources, without any correction of $[\eta]$ for shear-rate effects in the capillary viscometer used. More, the slope of $\log \eta_0$ vs $\log \bar{M}_v$ from Figure 8 in ref 43 is closer to 4 than to 3.4 and then would agree with the behavior shown in this work.

Then considering $\eta_{sp0} \sim C^2 M^4$, we replot the data in the form of $\log(\eta_{sp0}/M^4)$ vs $\log C$ (Figure 5). We can point out that all experimental data can be well explained if we assume a three-regime model: dilute, semidilute, and concentrated, as previously discussed by Takahashi et al.³⁵ and Colby et al.¹⁴ for flexible polymers. In the dilute regime, the Huggins law is valid and then it is limited by C_c^* . The semidilute regime can correspond to the linear dependence, in Figure 5, on which all the samples converge. In order to characterize the boundaries of this domain, the slope of the linear dependence is compared with those predicted for the semidilute regime by the theories for flexible polymers^{21,33,35} (Table III), assuming that they are applicable to semiflexible polymers. The agreement is good with the prediction from Takahashi et al.³⁵ giving $C^{4.35}$ variation for η_{sp0} . Consequently, this domain can be characterized by the single line of slope 4.35 that forms the experimental data for the different molecular weight

Table III. Comparison of the Experimental Concentration Dependence of the Viscosity ($\eta \propto C^\beta$) with Theoretical Predictions in 0.1 M NaCl

ν^{30}	β_{exp}^a	β^b	β^c	β^d
0.545	4 ± 0.2	3.6	4.35	3.72

^a Relation 3. ^b de Gennes,³³ $\beta = (6\nu - 1)/(3\nu - 1)$ (without hydrodynamic interactions). ^c Takahashi et al.,³⁵ $\beta = (4.4 - 3\nu)/(3\nu - 1)$. ^d Yamaguchi et al.,²¹ relation 29 in ref 21. ν : experimental exponent of $(\rho^2)^{1/2} \alpha M^\nu$.

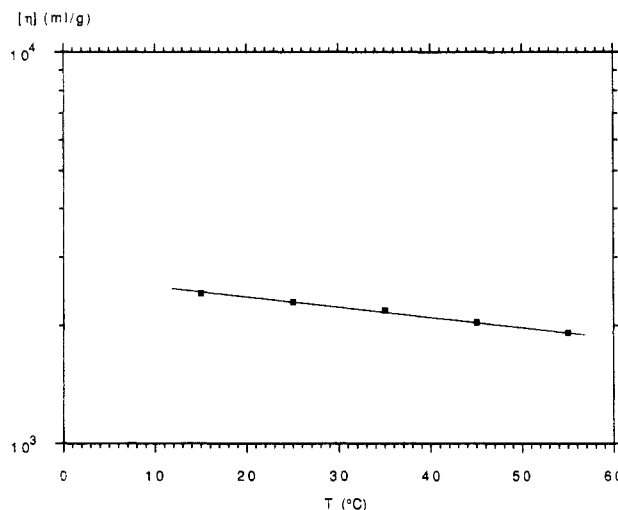


Figure 6. Temperature dependence of the intrinsic viscosity of H-2 in 0.1 M NaCl.

samples. The onset of the semidilute regime, particularly developed for the highest molecular weights, takes place at $C/C^* \simeq 10 \pm 1$, slightly higher than $C_c^*/C^* \simeq 6$, which characterizes the departure from the Huggins behavior.

The deviation of the experimental data from the scaling theory at higher concentrations is found to occur at a critical concentration C_c^{**} independent of molecular weight and equal to about 15 g/L. According to the definition given by Tinland et al.⁴² for the onset of the concentrated regime for a wormlike polymer (eq 19, ref 42) this regime should appear above concentrations equal to 15.7 g/L using the hyaluronate persistence length equal to 80 Å.³⁰ This value is in perfect agreement with the data in Figure 5. The model of Berry and Fox⁴⁶ is valid in this last domain, and like for polybutadiene,¹⁴ the β exponent is lower in this domain compared with the β value obtained in the semidilute regime. Measurements at higher concentrations are in progress in our laboratory in order to achieve a better characterization of the limits of the concentrated region, using different rheological measurements.

As obtained by Takahashi et al., the semidilute region is more extended for the highest molecular weights. The lower molecular weight sample (H-5) does not show the semidilute regime. Then, relation 1 can be applied and a hypothetical M_c in the melt was estimated from the intercept of the two linear parts of the plot $\log \eta_{sp0}$ vs $\log C$. It is found to be very low and equal to about 1500, a value in the range roughly estimated or calculated for other semirigid chains.^{44,45} Using relation 1 the $(M_c)_{sol}$ calculated for $C = 10$ g/L ($M_{wc} = 280\,000$) is very similar to that obtained by Yanaki and Yamaguchi⁴³ at this polymer concentration ($M_{vc} = 350\,000$) if we consider the different methods used for M_w and M_v determinations in both sets of data.

Temperature Dependence. The effect of the temperature, T , was tested only with the sample H-2 at 0.1 M NaCl concentration. In order to relate the influence

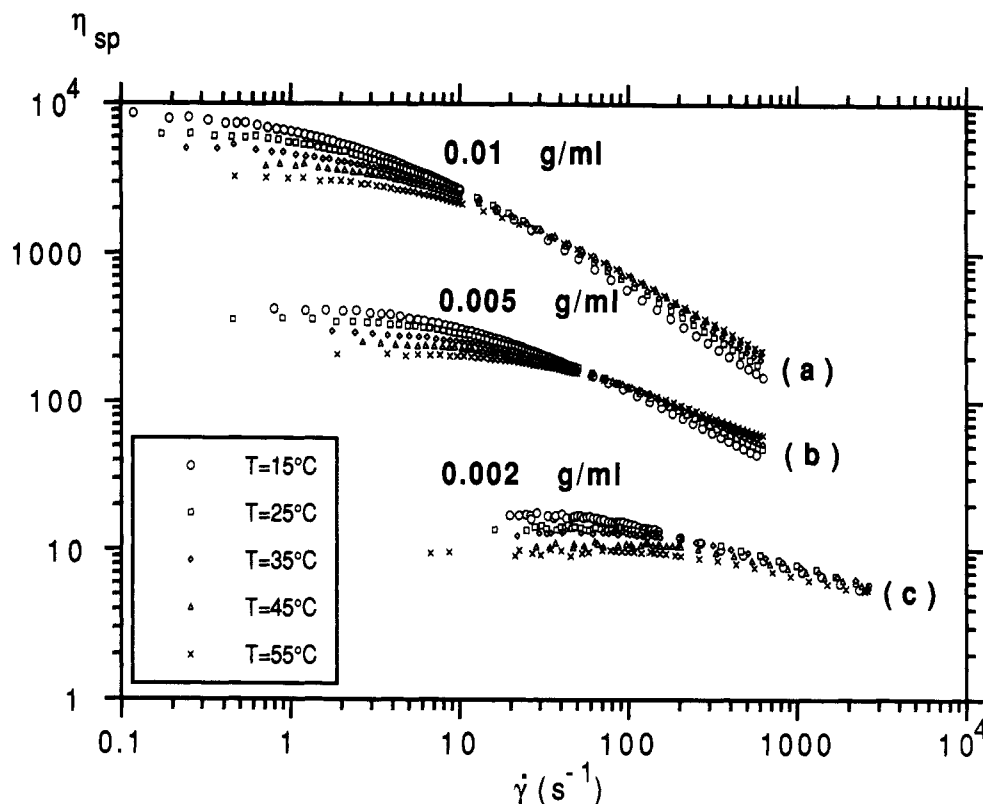


Figure 7. Temperature dependence of $\log \eta_{sp}$ vs $\log \dot{\gamma}$ for H-2 at (a) $C = 10^{-2}$, (b) $C = 5 \times 10^{-3}$, (c) $C = 2 \times 10^{-3}$ g/mL in 0.1 M NaCl.

of the temperature on $[\eta]$, Figure 6 shows $\log [\eta]$ vs T . The intrinsic viscosity decreases with increasing T with a temperature coefficient $d \ln [\eta]/dT$ of about -0.007 deg^{-1} , which is comparable with the range -0.007 to -0.008 deg^{-1} observed for other polysaccharides⁴⁷ but larger than the value found by Cleland in 0.02 M NaCl (-0.0044 deg^{-1}) for hyaluronates from bovine vitreous humor.⁴⁸ This difference could be attributed to the presence of intermolecular associations in the latter system. Figure 7 shows in a double-logarithmic plot the influence of the temperature on the viscosity as a function of $\dot{\gamma}$ for three polymer concentrations.

Considering the temperature dependence of η_0 , we do not find the sharp discontinuity at about 40°C reported by Morris et al.²² and our temperature dependence corresponds to that obtained above this temperature by these authors. According to their arguments no intermolecular segmental interactions are present in our samples even at low temperatures. This is perhaps another contribution of the protein content in hyaluronate from the animal source.

Shear-Rate Dependence on Viscosity. For dilute solutions the non-Newtonian regime when shear rate increases is relatively small and arises from alignment and deformation of transiently elongated chains in the direction of flow. For more concentrated solutions, shear thinning is much more dramatic, as illustrated in Figure 1, and arises also from an additional mechanism involving entanglements.¹⁰

It has been proposed to relate the onset of shear rate-viscosity dependence to the longest relaxation times in the solution. With the assumption that shear-rate dependence of viscosity is caused by a progressive decrease in the steady-state entanglement density, a relaxation time τ_{r0} can be defined in the dilute regime of flexible chains as^{10,12}

$$\tau_{r0} = 6\eta_s[\eta]M/\pi^2RT \quad (4)$$

where R is the gas constant and the coefficient $6/\pi^2$ is derived from the Rouse model of polymer dynamics. For a finite concentration $[\eta]$ can be replaced by $(\eta_0 - \eta_s)/\eta_s C$ and thus

$$\tau_r = 6(\eta_0 - \eta_s)M/\pi^2CRT \quad (5)$$

In this concept $\dot{\gamma}_c$, i.e. the critical shear rate where the viscosity becomes a function of $\dot{\gamma}$ is well expressed by τ_r^{-1} .

Therefore, if the extent of shear thinning (i.e. η/η_0) at a given shear rate is plotted against the product $\dot{\gamma}\tau_r$, knowing η_0 , M , C , and T , the viscosity-shear rate data for C , M , and T should be superposed. This behavior has been tested with success on a series of guar galactomannans.⁴⁹ In another way the product $\dot{\gamma}_c\tau_r$ should be constant of the order of 1, independent of C , M , and T .

Different ways have been proposed to determine the critical shear rate ($\dot{\gamma}_c$) corresponding to the onset of shear thinning. In this work $\dot{\gamma}_c$ was determined, for the highest molecular weights and concentrations, by extrapolation of the Newtonian plateau and the final slope of the shear thinning region in the log-log plot of η_{sp} vs $\dot{\gamma}$ (Figure 1). For the lowest concentrations and molecular weights we estimate $\dot{\gamma}_c$ from the coefficient of translation along the $\dot{\gamma}$ axis necessary to superpose in a double-logarithmic plot their ratio $\eta_{sp}(\dot{\gamma})/\eta_{sp0}$ with that obtained for the highest molecular weights (in the range of values between 1 and 0.6). The results are given in Figure 8 in a log-log plot. In the semidilute regime, the concentration dependences of $\dot{\gamma}_c$ are almost independent of molecular weight and $\dot{\gamma}_c \propto C^{-3}$. Figure 9 shows $\log \dot{\gamma}_c$ vs $\log \bar{M}_w$ in 0.1 M NaCl at $C = 10^{-2}$ g/mL. This figure reveals that $\dot{\gamma}_c \propto \bar{M}_w^{-4.8}$, in the semidilute regime. Then the dependence of $\dot{\gamma}_c$ with \bar{M}_w and C are approximately given in this regime by

$$\dot{\gamma}_c \propto C^{-3}\bar{M}_w^{-4.8} \quad (6)$$

These dependences are very similar to those predicted from relations 3 and 5, i.e., $\tau_r^{-1} \propto C^{-3}\bar{M}_w^{-5}$ if we assume $\dot{\gamma}_c$

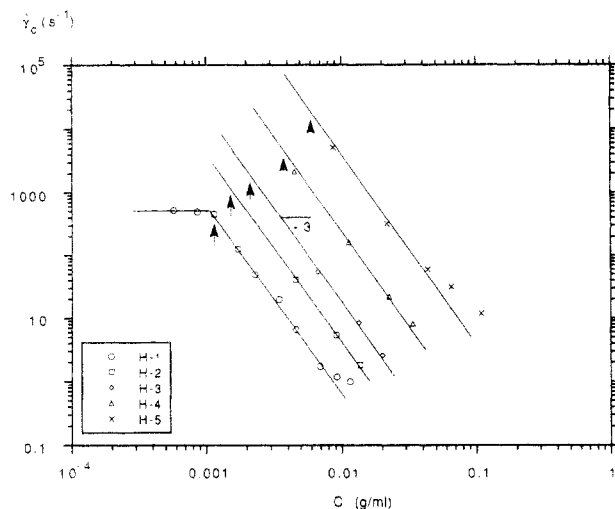


Figure 8. Variation of the critical shear rate, $\dot{\gamma}_c$, for the onset of shear thinning behavior as a function of hyaluronate concentration for the different samples in 0.1 M NaCl at 25 °C. Arrows indicate the critical concentration C_c^* (see text).

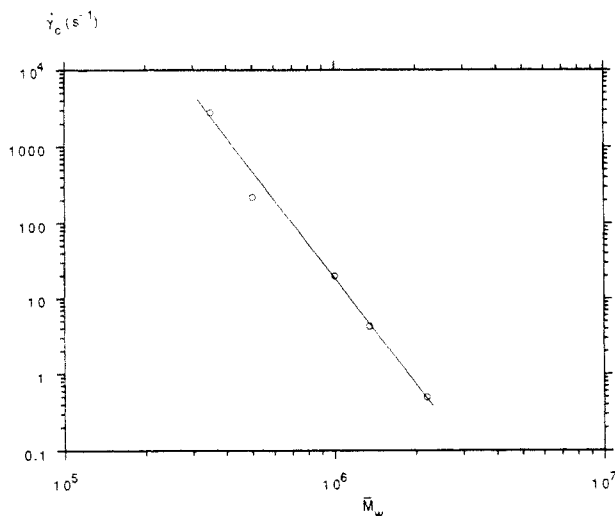


Figure 9. Molecular weight dependence of $\dot{\gamma}_c$ in 0.1 M NaCl at $C = 0.01$ g/mL and 25 °C.

Table IV. Comparison of $\dot{\gamma}_c$ with the Inverse of the Relaxation Time Calculated from Eq 5 for Different Temperatures and Concentrations in 0.1 M NaCl

$10^3 C$ (g/mL)		15 °C	25 °C	35 °C	45 °C	55 °C
2	$\dot{\gamma}_c$ (s ⁻¹)	91	167	216	326	
	τ_r^{-1} (s ⁻¹)	310	486	673	1033	1430
	$\dot{\gamma}_c \tau_r$	0.30	0.34	0.32	0.31	
5	$\dot{\gamma}_c$ (s ⁻¹)	12	18.6	26.2	43.2	62.2
	τ_r^{-1} (s ⁻¹)	31.2	47.9	74.8	114.3	158.3
	$\dot{\gamma}_c \tau_r$	0.38	0.38	0.36	0.38	0.4
10	$\dot{\gamma}_c$ (s ⁻¹)	2	3.1	4.5	7.2	10
	τ_r^{-1} (s ⁻¹)	3.2	5.3	8.7	13.4	21.1
	$\dot{\gamma}_c \tau_r$	0.62	0.59	0.53	0.53	0.47

$\propto \tau_r^{-1}$. To compare these two last values, the product $\dot{\gamma}_c \tau_r$ calculated for different temperatures is given in Table IV and for different concentrations and molecular weights in Table V. These values vary randomly from 0.3 to 2 probably as a consequence of the lack of precision in the determination of $\dot{\gamma}_c$. These results confirm that τ_r^{-1} calculated from relation 5 gives a good approximation of the critical shear rate of the onset of shear thinning behavior, taking into account the concentration, temperature, and molecular weight dependences.

In the dilute regime, except for the highest molecular weight (sample H-1), it was not possible to extract directly the critical shear rate of the beginning of shear thinning,

Table V. Critical Shear Rate, $\dot{\gamma}_c$, τ_r^{-1} (Eq 5), and $\dot{\gamma}_c \tau_r$ Products for the Different Samples at Different Concentrations in 0.1 M NaCl at 25 °C

sample	$10^3 C$ (g/mL)	$\dot{\gamma}_c$ (s ⁻¹)	τ_r^{-1} (s ⁻¹)	$\dot{\gamma}_c \tau_r$
H-1	10	1	0.5	2
	8	1.2	0.9	1.3
	6	1.7	2.2	0.8
	4	6.7	9.5	0.7
	3	20	22	0.9
	2	50	56	0.9
	1.5	128	90	1.4
	1	354	167	2.0
	0.75	400	209	1.9
	0.5	526	278	1.9
H-2	13.7	1.8	1.6	1.1
	9.12	5.3	6.1	0.9
	4.56	28	4.8	0.6
	1.82	130	274	0.5
	0.91	280	527	0.5
H-3	20	2.6	2.2	1.2
	13.4	8.5	8.8	1.0
	6.7	55.1	68	0.8
	2.7	364	464	0.8
H-4	33.7	8.2	18	0.5
	22.5	22.2	60	0.4
	11.2	164	370	0.4
	4.5	2160	1928	1.1
H-5	65.1	31.3	20	1.6
	43.4	59.7	65	0.9
	21.7	321	422	0.7

$\dot{\gamma}_{c0} : (\tau_{r0})^{-1}$ (s⁻¹)

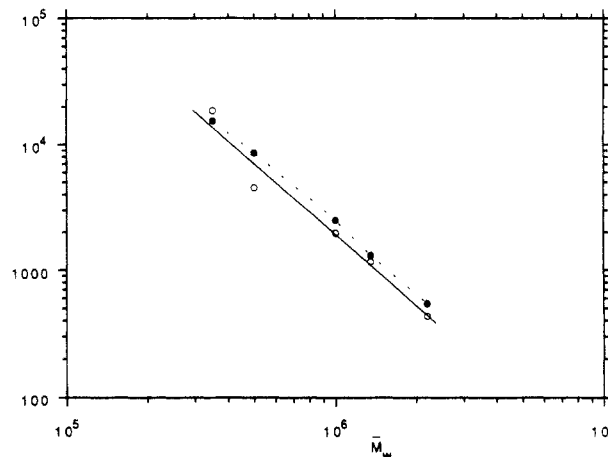


Figure 10. Dependence of the critical shear rate, $\dot{\gamma}_{c0}$, determined in the dilute regime versus \bar{M}_w for the different samples in 0.1 M NaCl solutions at 25 °C (open circles). Comparison with calculated τ_{r0}^{-1} (eq 4, filled circles).

$\dot{\gamma}_{c0}$. This is due to the fact that the rheometers used are not sensitive enough to reach the shear thinning behavior. For this sample, $\dot{\gamma}_{c0}$ appears to be constant up to a critical concentration C_c^* , similar to that determined from viscosity (Figure 8 and Table I). Assuming the same behavior for the other samples, we were able to determine $\dot{\gamma}_{c0}$ by extrapolation of $\dot{\gamma}_c$ to C_c^* (Figure 8). Figure 10 shows the dependence of $\dot{\gamma}_{c0}$ with \bar{M}_w together with τ_{r0}^{-1} values calculated from eq 4. It predicts $\tau_{r0}^{-1} \propto C^0 M^{-1.80}$ by using the Mark-Houwink exponent $a = 0.8$.³⁰ Experimental dependence shows $\dot{\gamma}_{c0} \propto C^0 M^{-1.76}$ (Figure 10). Consequently, the inverse of the longest relaxation time in solution, which should be related to the motion of the chains, appears to be a good estimate of the critical shear rate of the onset of shear thinning behavior in dilute and more concentrated solutions. Then, eqs 4 and 5 where the effect of stiffness is included through the viscosity may be applied to semirigid polymers, as previously mentioned.⁴⁹

Conclusion

There are very few papers which describe the rheological properties of polyelectrolytes and wormlike polymers, and the available results are sometimes conflicting. Intermolecular associations are perhaps the major cause of these discrepancies. Nevertheless, at present, these polymers have a growing interest for fundamental studies and industrial applications. Hyaluronate is one of these polymers. In this work, from very well characterized samples of different molecular weights, the flow behavior of hyaluronate solutions was studied and some differences in comparison with flexible polymers were observed. One of them is the low concentrations for appearance of entanglement in solution characterized by the CM_c product equal to about 2800 (g/mL) which is about 10 times lower than those found for flexible polymers in solution.¹⁰ Another difference is a greater dependence of zero-shear viscosity on molecular weight (M^4 instead of $M^{3.4}$ for flexible polymers). At present no theoretical model predicts this dependence. Concerning the influence of polymer concentration on the zero-shear viscosity the data were analyzed on the basis of the scaling concept of de Gennes. The theory was found to be useful for clarifying the range of the semidilute region, and it is shown that this theory, developed for flexible chains, can be applied to wormlike chains. The results are similar to those found by Takahashi et al. on poly(α -methylstyrene) and Colby et al. on polybutadiene, two flexible polymers.

The onset of shear thinning behavior is well defined by the inverse of the longest relaxation time in solution, τ_r^{-1} , regardless of the conditions, but in contrast with flexible polymers the shear thinning behavior appears at very low shear rate. This is only due to the relatively high intrinsic viscosities of these polymers. At the end, the differences obtained with results published for hyaluronate of animal sources were attributed to the higher protein content in the latter, leading to intermolecular associations.

Acknowledgment. We thank Professor M. Benmouna for fruitful discussions and valuable comments, the reviewer for helpful suggestions which contributed to the improvement of the paper, and F. Launay and R. de Baynast from the laboratoires ARD (Royallieu III, rue du Docteur Alexis Carrel, F-60200 Compiègne) for the financial support, the scientific cooperation, and gift of samples.

References and Notes

- (1) Asheim, A.; Lindbald, G. *Acta Vet. Scand.* **1976**, *17*, 379.
- (2) Numiki, O.; Toyoshima, M.; Morisaki, N. *Clin. Orthop.* **1982**, *146*, 260.
- (3) Miller, D.; Stegmann, R., Eds. *Healon (sodium hyaluronate) A guide to its use in ophthalmic surgery*; Wiley: New York, 1983.
- (4) Balazs, E. A.; Band, P. *Cosmet. Toiletries* **1984**, *99*, 65.
- (5) Reed, W. F.; Ghosh, S.; Medjahdi, G.; François, J. *Macromolecules* **1991**, *24*, 6189.
- (6) Wang, L.; Bloomfield, V. A. *Macromolecules* **1991**, *24*, 5791.
- (7) Nordmeier, E.; Dauwe, W. *Polym. J.* **1992**, *24*, 229.
- (8) Fenley, M. O.; Manning, G. S.; Olson, W. K. *J. Phys. Chem.* **1992**, *96*, 3963.
- (9) Förster, S.; Schmidt, M.; Antonietti, M. *J. Phys. Chem.* **1992**, *96*, 4008.
- (10) Graessley, W. W. *Adv. Polym. Sci.* **1974**, *16*, 1.
- (11) De Gennes, P. G. *Scaling concepts in polymer physics*; Cornell University Press: Ithaca, NY, 1979.
- (12) Ferry, J. D. *Viscoelastic properties of polymers*, 3rd ed.; Wiley: New York, 1980.
- (13) Kulicke, W. M.; Kniewske, R. *Rheol. Acta* **1984**, *23*, 75.
- (14) Colby, R. H.; Fetters, L. J.; Funk, W. G.; Graessley, W. W. *Macromolecules* **1991**, *24*, 3873.
- (15) Matheson, J. *Macromolecules* **1980**, *13*, 643.
- (16) Erman, B.; Bahar, I.; Navard, P. *Macromolecules* **1989**, *22*, 358.
- (17) Sato, T.; Teramoto, A. *Macromolecules* **1991**, *24*, 193.
- (18) Morris, E. R.; Cutler, A. N.; Ross-Murphy, S. B.; Rees, D. A.; Price, J. *Carbohydr. Polym.* **1981**, *1*, 5.
- (19) Milas, M.; Rinaudo, M.; Knipper, M.; Schuppiser, J. L. *Macromolecules* **1990**, *23*, 2506.
- (20) Takada, Y.; Sato, T.; Teramoto, A. *Macromolecules* **1991**, *24*, 6215.
- (21) Yamaguchi, M.; Wakutsu, M.; Takahashi, Y.; Noda, I. *Macromolecules* **1992**, *25*, 470.
- (22) Morris, E. R.; Rees, D. A.; Welsh, E. J. *J. Mol. Biol.* **1980**, *138*, 383.
- (23) Welsh, E. J.; Rees, D. A.; Morris, E. R.; Madden, J. K. *J. Mol. Biol.* **1980**, *138*, 375.
- (24) Ribitsch, G.; Schurz, J.; Ribitsch, V. *Colloid Polym. Sci.* **1980**, *258*, 1322.
- (25) Sheehan, J. K.; Arundel, C.; Phelps, C. F. *Int. J. Biol. Macromol.* **1983**, *5*, 222.
- (26) Gibbs, D. A.; Merrill, E. W.; Smith, K. A.; Balazs, E. A. *Biopolymers* **1968**, *6*, 777.
- (27) Reed, C. E.; Li, X.; Reed, W. F. *Biopolymers* **1989**, *28*, 1981.
- (28) Ghosh, S.; Li, X.; Reed, C. E.; Reed, W. F. *Biopolymers* **1990**, *30*, 1101.
- (29) Cleland, R. L. *Biopolymers* **1984**, *23*, 647.
- (30) Fouissac, E.; Milas, M.; Rinaudo, M.; Borsali, R. *Macromolecules* **1992**, *25*, 5613.
- (31) Tinland, B.; Mazet, J.; Rinaudo, M. *Makromol. Chem. Rapid Commun.* **1988**, *9*, 69.
- (32) Graessley, W. W. *Polymer* **1980**, *21*, 258.
- (33) De Gennes, P. G. *Macromolecules* **1976**, *9*, 587.
- (34) Berry, G. C.; Nakayasu, H.; Fox, T. G. *J. Polym. Sci., Polym. Phys. Ed.* **1979**, *17*, 1825.
- (35) Takahashi, Y.; Isono, Y.; Noda, I.; Nagasawa, M. *Macromolecules* **1985**, *18*, 1002.
- (36) Takahashi, Y.; Noda, I.; Nagasawa, M. *Macromolecules* **1985**, *18*, 2220.
- (37) Cleland, R. L.; Wang, J. L. *Biopolymers* **1970**, *9*, 799.
- (38) Castelain, C.; Doublier, J. L.; Lefebvre, J. *Carbohydr. Polym.* **1987**, *7*, 1.
- (39) Ganter, J.; Milas, M.; Correa, J. B. C.; Reicher, F.; Rinaudo, M. *Carbohydr. Polym.* **1992**, *17*, 171.
- (40) Gravanis, G.; Milas, M.; Rinaudo, M.; Clarke-Sturman, A. J. *Int. J. Biol. Macromol.* **1990**, *12*, 201.
- (41) Campana, S.; Andrade, C.; Milas, M.; Rinaudo, M. *Int. J. Biol. Macromol.* **1990**, *12*, 379.
- (42) Tinland, B.; Maret, G.; Rinaudo, M. *Macromolecules* **1990**, *23*, 596.
- (43) Yanaki, T.; Yamaguchi, T. *Biopolymers* **1990**, *30*, 415.
- (44) Aharoni, S. M. *Macromolecules* **1986**, *19*, 426.
- (45) Zang, Y. H.; Carreau, P. J. *J. Appl. Polym. Sci.* **1991**, *42*, 1965.
- (46) Berry, G. C.; Fox, T. G. *Adv. Polymer Sci.* **1968**, *5*, 261.
- (47) Milas, M.; Rinaudo, M. *Carbohydr. Res.* **1986**, *158*, 191.
- (48) Cleland, R. L. *Biopolymers* **1979**, *18*, 1821.
- (49) Robinson, G.; Ross-Murphy, S. B.; Morris, E. D. *Carbohydr. Res.* **1982**, *107*, 17.